Meteoritics & Planetary Science 35, 95–106 (2000)

Petrology and chemistry of the new shergottite Dar al Gani 476

J. ZIPFEL*, P. SCHERER, B. SPETTEL, G. DREIBUS AND L. SCHULTZ

Max-Planck-Institut für Chemie, Abteilung Kosmochemie, Postfach 3060, 55020 Mainz, Germany
Correspondence author's e-mail address: zipfel@mpch-mainz.mpg.de

(Received 1999 March 12; accepted in revised form 1999 September 16)

Abstract–In 1998, Dar al Gani (DaG) 476 was found in the Libyan desert. The meteorite is classified as a basaltic shergottite and is only the 13th martian meteorite known to date. It has a porphyritic texture consisting of a fine-grained groundmass and larger olivines. The groundmass consists of pyroxene and feldspathic glass. Minor phases are oxides and sulfides as well as phosphates. The presence of olivine, orthopyroxene, and chromite is a feature that DaG 476 has in common with lithology A of Elephant Moraine (EET) A79001. However, in DaG 476, these phases appear to be early phenocrysts rather than xenocrysts. Shock features, such as twinning, mosaicism, and impact-melt pockets, are ubiquitous. Terrestrial weathering was severe and led to formation of carbonate veins following grain boundaries and cracks.

With a molar MgO/(MgO + FeO) of 0.68, DaG 476 is the most magnesian member among the basaltic shergottites. Compositions of augite and pigeonite and some of the bulk element concentrations are intermediate between those of lherzolitic and basaltic shergottites. However, major elements, such as Fe and Ti, as well as LREE concentrations are considerably lower than in other shergottites.

Noble gas concentrations are low and dominated by the mantle component previously found in Chassigny. A component, similar to that representing martian atmosphere, is virtually absent. The ejection age of 1.35 ± 0.10 Ma is older than that of EETA79001 and could possibly mark a distinct ejection.

INTRODUCTION

A chemically well-defined group of 12 meteorites is believed to come from Mars (McSween, 1994; Bogard and Johnson, 1983). This is primarily because shock-implanted noble gases and N in impact-melt inclusions in some of these meteorites closely match the composition and isotopic properties of martian atmospheric gases, as determined by the *Viking* lander in the 1970s (Bogard and Johnson, 1983; Wiens *et al.*, 1986).

The diversity of lithologies and compositions represented by these meteorites allows one to model the geochemical and geological evolution of Mars. Basaltic shergottites—Shergotty, Zagami, Queen Alexandra Range (QUE) 94201, Elephant Moraine (EET) A79001—are pyroxene-rich igneous rocks that probably formed either in near-surface dykes or in larger lava flows. On the other hand, lherzolitic shergottites—Allan Hills (ALH) A77005, Lewis Cliff (LEW) 88516, and Yamato (Y)-793605—have cumulate textures, greater proportions of olivine, and lower proportions of feldspathic glass, and formed in plutonic environments. Other martian meteorites also have cumulate textures and were formed in plutonic environments. There are three clinopyroxene cumulates (Nakhla, Lafayette, Governador Valadares), one olivine cumulate (Chassigny), and one orthopyroxene cumulate (ALH 84001). The findings of possible evidence for traces of life on Mars in ALH 84001 and Nakhla raised the question of biological activity on Mars (McKay *et al.*, 1996, 1999).

On 1998 May 1, the 13th martian meteorite was recovered in the Dar al Gani region of the Libyan Sahara and is named Dar al Gani (DaG) 476. Here we present a study of the new martian meteorite's bulk chemistry, mineralogy, and noble gas inventory. Our results allow us to classify this meteorite as a basaltic shergottite. The study of DaG 476 constrains formation processes of mafic-rich lithologies among basaltic shergottites.

First results of the mineralogy and bulk chemistry of DaG 476 were published by Zipfel *et al.* (1999) and Mikouchi (1999). The recently recognized basaltic shergottite DaG 489 has similar properties and is paired with DaG 476 (Folco *et al.*, 1999).

METHODS

During the course of this study, eight thin sections were prepared and examined with an optical microscope. Two sections were studied with the backscattered electron detector of the JEOL Superprobe (Johannes Gutenberg-Universität, Mainz and Humboldt Universität, Berlin), which was also used to perform quantitative mineral analyses in the wavelength dispersive mode.

Mineral modes of two thin sections (#1 and #7) were derived by point counting (Table 1). Under the optical microscope, 1068 points were counted in thin section #1, which has an area of 50 mm^2; abundances of pigeonite, augite, and orthopyroxene were determined from microprobe analyses of 105 randomly selected pyroxenes. On a mosaic of backscattered electron images, 9434 points were counted in thin section #7, which has an area of 75 mm^2. Although contrast was optimized in these images, it was not possible to reliably distinguish augite from pigeonite. However, magnesian-rich orthopyroxene cores could easily be recognized. The mineral modes of the two thin sections are in good agreement with one another, which indicates that the meteorite has a homogeneous composition.

Electron microprobe analyses of olivine and pyroxenes were done with a focused beam at 15 kV and 12 nA. During analyses of feldspathic glasses, the beam was defocused to 5 or 10 μm at measurement conditions of 15 kV and 15 nA. Oxides were analysed with a focused beam at 20 kV and 12 nA. Calibrations of all measurement conditions were based on synthetic and natural standards and repeatedly checked with natural standards. Data reduction followed the Phi-Rho-Z procedure. Results of representative microprobe analyses are shown in Table 2.

Two sets of samples, one surface sample (66.1 mg) and one sample from the interior of the meteorite (about 2–3 cm from the surface), were prepared for instrumental neutron activation analyses (INAA). From the latter, a 5 g sample was crushed and subsequently powdered in an agate mill in order to ensure sample homogeneity. An aliquot (191.5 mg) of this powder and the exterior sample were irradiated in the Triga Mark II Reactor of Johannes Gutenberg-

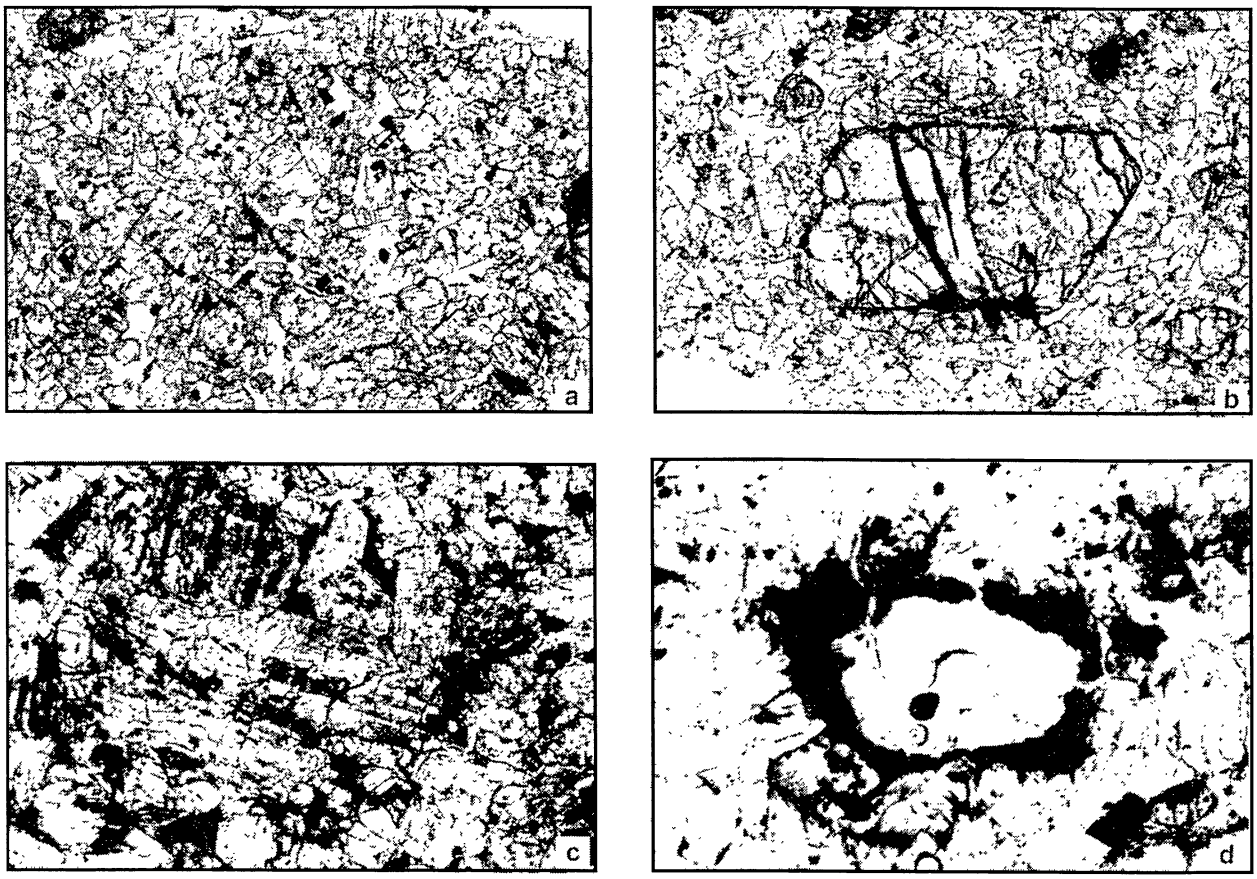

FIG. 1. Transmitted light photomicrographs. (a) Typical texture of the fine-grained groundmass that consists of granular and lath-shaped pyroxenes, interstitial feldspathic glass (white), and black opaques. (b) A large subhedral olivine sitting in the fine-grained groundmass. (c) The central elongated pyroxene has a dark orthopyroxene core. (d) Fresh impact melt with a central hole (gas bubble?). The dark rim consists of recrystallized glass. Fields of view are 1.8 × 2.3 mm for (a) and (b), and 0.9 × 1.15 mm for (c) and (d).

Universität, Mainz, at a neutron flux of 7×10^{11} n cm^{-2} s^{-1}. In addition, major elements were determined on two aliquots of the same powder by x-ray fluorescence spectroscopy (XRF) at Universität zu Köln. The precision of the XRF analyses is estimated to be better than 1–2 rel%. Concentrations of S and C of a 200 mg aliquot of the powder were analyzed by a C and S analyzer following described procedures (Dreibus *et al.*, 1995). Results are presented in Tables 3 and 4.

Abundance and isotopic composition of He, Ne, Ar, as well as the concentrations of ^{84}Kr, ^{129}Xe, and ^{132}Xe were determined in five whole-rock samples with the MAP 215 noble gas mass spectrometer "Alfred" following procedures described by Loeken *et al.* (1992). Results are given in Table 5.

PETROGRAPHY

Dar al Gani 476 is a meteorite fragment with an elongated shape (roughly 15 by 10 cm in size) and a total weight of 2015 g. Its surface is free of fusion crust, apparently due to wind erosion. The part that was lying on the soil is partially covered with the terrestrial desert weathering product, caliche. Otherwise, the surface has a smooth brown color, evenly speckled with larger dark to brownish spots (olivine grains). A 4 cm thick end piece was sliced several times, and freshly cut surfaces are greenish to brownish in color. A long carbonate vein of at least 2 mm thickness is visible on the cut surface of the main mass and on surfaces of individual slices. At the contact with this vein, the meteorite is discolored.

Dar al Gani 476 has a porphyritic texture consisting of a fine-grained groundmass and larger olivine grains (Fig. 1a,b). Olivines in DaG 476 typically range in size from 100 μm to 2 mm and have euhedral or anhedral shapes. Large olivines appear to be weakly aligned. Mostly, they occur as isolated grains but some form clusters of two or more grains. Some olivines have reacted with the groundmass, as indicated by ragged and embayed grain boundaries. In addition, they contain inclusions consisting of a Si, Al-rich glass, and fine crystallites of augite, olivine, and Ti-chromite. Others contain, either in inclusions or along cracks, pigeonite intergrown with Ti-chromite. Tiny (micron-sized) inclusions of chromites, which are typically mantled by pyroxene, are present in larger olivines (see also Fig. 4). Megacryst assemblages of olivine, orthopyroxene, and chromite common in lithology A of EETA79001 (McSween and Jarosewich, 1983; Steele and Smith, 1982) are not observed in DaG 476.

The fine-grained groundmass has an average grain size of 130 μm and consists mainly of pyroxene of granular or lath-like shapes and interstitial feldspathic glass (formerly plagioclase). Pyroxene is mostly pigeonite. Minor augite and orthopyroxene are present. Augite occurs either as individual grains, as cores of pyroxene grains mantled by pigeonite, or as overgrowths on pigeonite cores. Orthopyroxene occurs as patches in pigeonite cores (Fig. 1c). Minor phases are chromite, titanian chromite, ilmenite, sulfides, and phosphates. Phosphates are mostly whitlockite. Only one grain of Cl-apatite was found. Sulfides are Fe-sulfides with tiny Ni-rich exsolutions (probably pentlandite).

Shock features such as planar deformation faults, shock twinning, and mosaicism are present in olivines and pyroxenes. Former feldspar is now optically isotropic, probably due to shock, and is referred to as feldspathic glass throughout the text. Large pockets (up to 1 mm) of brownish colored recrystallized impact melt, darkened by extremely fine-grained Fe-rich phases, are abundant and found in association with pyroxene or olivine. Of all impact-melt pockets present, only a few were found to consist of fresh unrecrystallized glass of green and white color (Fig. 1d). In the center of these fresh glasses are spherical holes formed probably by gas bubbles. Carbonates are preferentially associated with these impact-melt pockets.

Carbonate ($CaCO_3$) veins are abundant, following grain boundaries and cracks. Most likely they formed during terrestrial weathering. Rare grains of $BaSO_4$, typically associated with these carbonates, are present and also probably formed during terrestrial weathering.

Modes of pyroxene, feldspathic glass, olivine, opaques, and others are shown in Table 1; other minerals include phosphates, impact-melt pockets, and carbonates; mesostasis was not observed. Also in Table 1, modes of DaG 476 are compared to modes of lithology A and B in EETA79001 as given by McSween and Jarosewich (1983). The high modal abundance of feldspathic glass (14–17 vol%) allows classification of DaG 476 as a basaltic shergottite (Treiman *et al.*, 1994). The high abundance of olivine (15–17 vol%) in DaG 476 is unusual. Only traces of olivine are present in the basaltic shergottites QUE 94201 (McSween *et al.*, 1996), Shergotty (Stolper and McSween, 1979), and Zagami (Stolper and McSween, 1979; McCoy *et al.*, 1999), with the exception of late stage melt pockets of the latter, which have a high abundance of extremely Fe-rich olivine. The only other basaltic shergottite with a significant proportion of olivine (7–13 vol%) is lithology A of EETA79001 (McSween and Jarosewich, 1983; Steele and Smith, 1982).

TABLE 1. Modal composition of DaG 476 and EETA79001.

	DaG 476			EETA79001	
	section #1 vol%	section #7 vol%	DaG 476 range* vol%	A† vol%	B† vol%
Pyroxene	58	60	60–62	69–73	56–66
Pigeonite	*52*	–	*53–?*	*55–63*	*32–54*
Augite	*2.8*	–	*2.9–?*	*3.2–8.5*	*12–25*
Orthopyroxene	*3.4*	*1.5*	*1.5–3.5*	*3.4–7.2*	–
Olivine	14	17	15–17	7–10	–
Feldspathic glass	17	14	14–17	16–18	28–30
Opaques	3.8	2.6	2.7–3.9	2.2–4.0	3.4–3.8
Chromite					
Ti-chromite					
Ilmenite					
Fe-sulfide					
Phosphates	tr	tr	tr	tr–0.4	0.2–0.7
Mesostasis	–	–	–	tr–0.3	0.5–1.1
Impact-melt pockets	4.5	4.0	4.1–4.6	–	–
Carbonate	2.7	2.2	–	–	–

*Range of sections #1 and #7 with carbonate normalized out.
†Lithology A and B of EETA79001 (McSween and Jarosewich, 1983).

MINERAL COMPOSITION

Results of representative mineral analyses are shown in Table 2. Compositions of pyroxenes, olivine, and feldspathic glass are illustrated in Fig. 2.

Feldspathic glasses are Ca-rich (An_{52}–An_{72}), which is more anorthitic than those in lithology A of EETA79001 (An_{50-65}) and other shergottites (McSween and Jarosewich, 1983; Steele and Smith, 1982). No correlation between core and rim composition was found. Single grains appear to be of homogeneous composition.

Pyroxene is mostly clinopyroxene, consisting of pigeonite and minor augite. Orthopyroxene occurs as cores of pigeonite grains. Some of these orthopyroxenes are optically distinguishable from pigeonite and augite by low birefringence and the absence of shock twins, but not all show these properties. Because of this uncertainty in the optical identification of orthopyroxene, and because there is a continuous trend of $Wo_{1.7}$ to $Wo_{14.2}$, orthopyroxenes and pigeonites were differentiated based on compositions below and above Wo_5, respectively.

Orthopyroxene typically is magnesian, ranging in composition from $Fs_{18.3-24.6}Wo_{1.6-5.0}$. One grain analyzed, however, has an unusual composition of $Fs_{28.9}Wo_{4.5}$ (Figs. 2 and 3). Pigeonite compositions ($Fs_{22.2-33.7}Wo_{5.5-14.2}$) overlap with the low-Fs end of the pigeonite trend of EETA79001 lithology A but do not extend to the more Fs-rich compositions of that trend (Fig. 2). In comparison to other shergottites, augite compositions ($Fs_{17-21}Wo_{29-35}$) fall in the compositional gap between lherzolitic shergottites and lithology A of EETA79001. Pyroxenes are zoned, with respect to Fe and Mg, with a subtle increase of Fe towards the rim. Coexisting pigeonite and augite pairs appear to be in equilibrium at temperatures between 1100 and 1200 °C (Lindsley, 1983). This pyroxene temperature may reflect crystallization temperatures.

Concentrations of the minor elements TiO_2, Cr_2O_3, Al_2O_3, and CaO are plotted against the molar Fe/(Fe + Mg) (fe-number) in Fig. 3. Each symbol represents a single analysis. Typically, we analyzed the core and rim of a single grain twice. In addition, the range of molar Fe/(Fe + Mg) ratios in olivines are shown.

The fe-numbers of orthopyroxenes are lower than for pigeonite, augite, and olivine and range from 0.17 to 0.27. Concentration of TiO_2 is low and constant over the whole Fe-range, whereas CaO concentrations increase with increasing Fe. Although concentrations of Al_2O_3 and Cr_2O_3 scatter, there is one observation worth mention-

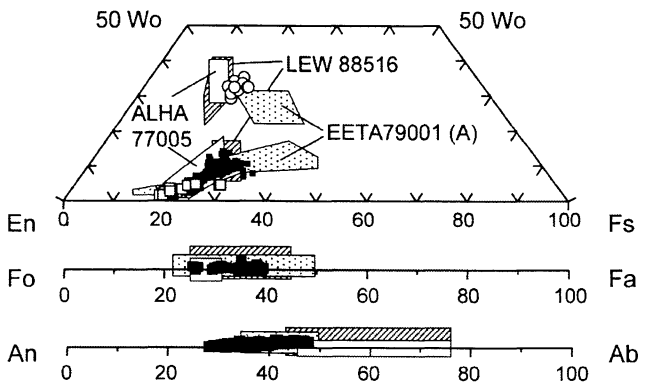

FIG. 2. Chemical compositions of orthopyroxene, pigeonite, augite, olivine, and feldspathic glass. Symbols represent analyses in DaG 476. Pyroxene symbols are orthopyroxene (open squares), augite (open circles), and pigeonite (filled squares). Shaded areas indicate compositional fields of lithology A of basalt EETA79001, and of the lherzolites ALHA77005 and LEW 88516. Sources of data are Harvey *et al.* (1993), Lundberg *et al.* (1990), McSween *et al.* (1979), McSween and Jarosewich (1983), Steele and Smith (1982), and Treiman *et al.* (1994).

TABLE 2. Representative electron microprobe analyses of major minerals.

	Ortho-pyroxene	Olivine		Pigeonite		Augite		Feldsp. glass
		Fa-poor	Fa-rich	core	rim	core	rim	
SiO_2	56.0	37.9	36.3	54.1	53.0	52.2	51.6	51.2
TiO_2	–	–	–	0.14	0.16	0.35	0.71	–
Al_2O_3	0.32	–	–	0.76	1.05	1.76	1.53	29.3
Cr_2O_3	0.44	–	–	0.42	0.54	0.73	0.65	–
FeO†	12.2	23.5	34.2	16.0	17.3	11.4	12.9	0.38
MnO	0.45	0.48	0.70	0.53	0.59	0.40	0.47	–
MgO	29.9	37.4	29.6	24.1	22.1	17.4	16.3	0.21
CaO	0.84	0.31	0.20	3.84	5.36	15.8	15.7	14.0
Na_2O	–	–	–	0.08	0.09	0.21	0.25	3.58
K_2O	–	–	–	–	–	–	–	0.05
Total	100.2	99.9	101.2	100.0	100.2	100.4	100.2	98.8
Fa	–	26.1	39.3	–	–	–	–	–
Fs/Ab	18.3	–	–	25.1	27.2	18.2	17.1	31.5
Wo/Or	1.6	–	–	7.7	10.8	32.2	34.2	0.3
En/An	80.1	–	–	67.2	62.0	49.5	48.7	68.2

	Chromite		Ti-chromite		Ilmenite	Phosphates		Impact-melt average
	inclusions in olivine	matrix	matrix					
SiO_2	–	–	–	–	–	–	–	46.1
TiO_2	0.94	1.46	18.9	20.6	52.9	n.d.	n.d.	1.53
Al_2O_3	9.11	9.92	5.62	6.87	–	n.d.	n.d.	1.61
V_2O_3	0.48	0.54	0.47	0.60	0.20	n.d.	n.d.	n.d.
Cr_2O_3	55.9	54.1	25.0	15.0	0.52	–	–	n.d.
FeO†	28.8	29.3	44.8	52.1	40.8	1.33	0.46	21.2
MnO	0.51	0.48	0.68	0.67	0.85	–	–	0.64
MgO	4.52	4.80	4.31	3.49	4.41	2.48	–	19.5
ZnO	0.10	0.08	0.07	0.07	–	n.d.	n.d.	n.d.
CaO	n.d.	n.d.	n.d.	n.d.	n.d.	47.1	52.3	5.29
Na_2O	n.d.	n.d.	n.d.	n.d.	n.d.	1.53	0.40	0.18
K_2O	n.d.	n.d.	n.d.	n.d.	n.d.	–	–	–
P_2O_5	n.d.	n.d.	n.d.	n.d.	n.d.	44.8	40.7	1.03
Cl	–	–	–	–	–	–	1.61	n.d.
Total	100.4	100.6	99.9	99.4	99.8	97.5	95.8	97.1

†Total Fe as FeO.
n.d. = not determined.

ing. At an fe-number of 0.20, both Cr and Al concentrations show a peak. Two analyses from the same grain indicate the presence of orthopyroxene even at a high fe-number of 0.30. With respect to Cr_2O_3, Al_2O_3 and CaO, the grain's composition lies on the extension of the trends defined by low-Fe orthopyroxenes. The TiO_2 concentration of this grain, however, is high for an orthopyroxene and even higher than that of pigeonite at the given fe-number.

In terms of fe-number, the onset of augite and pigeonite overlaps with Fe-rich orthopyroxene compositions and starts at a fe-number of ~0.24. This is close to the lowest fe-number of 0.26 found in two olivine cores. This indicates that the most magnesian olivine is almost in equilibrium with the most magnesian pigeonite and augite compositions but is not in equilibrium with the most magnesian orthopyroxene. There is evidence, however, that Fa_{26} in olivine is not necessarily a lower limit for olivines (see below). The augite trend covers a range of fe-numbers from 0.24 to 0.30. Over this range, TiO_2 strongly increases and Cr_2O_3 and Al_2O_3 decrease with increasing Fe, whereas CaO concentrations are high and constant. Pigeonite crystallized over a wider range of fe-numbers (0.24 to 0.37). Up to a fe-number of 0.33, concentrations of CaO, Al_2O_3, and Cr_2O_3 are nearly constant but decrease at higher Fe. The increase of TiO_2 with increasing fe-number in pigeonites is small between fe-number 0.25 and 0.30 but increases strongly at fe-numbers above 0.30.

Olivines can be divided into two chemical types: olivines with Mg-rich cores ($Fa_{min.\ 26}$), which are concentrically zoned to Fe-rich rims ($Fa_{\sim 38}$) (Fig. 4); and Fe-rich olivines ($Fa_{\sim 36}$, $_{\sim 38}$, and $_{\sim 39}$), which are chemically unzoned. These latter olivines are on average smaller than the zoned ones. In Fig. 5, results of the analyses of all olivines present in one thin section are shown. Each symbol represents an average, from at least two analyses, of Fa concentrations in the olivine core and rim. Core and rim analyses from single grains are connected by tie lines, when the compositional difference is large. Unzoned olivine grains have core and rim compositions at $Fa_{\sim 36}$ and between Fa_{38} and Fa_{39}. Rims of chemically zoned olivines scatter over a range of Fa_{34} to Fa_{38}. There is no dependence of rim composition on core composition, nor on size, composition of neighbouring phases, or depth of embayment. Therefore, it seems that all rim compositions may have a Fa of 38 and that lower rim Fa concentrations are artifacts of the grain sectioning. The distribution of olivine core Fa compositions of chemically zoned olivines, however, shows a systematic grouping. Three groupings can be

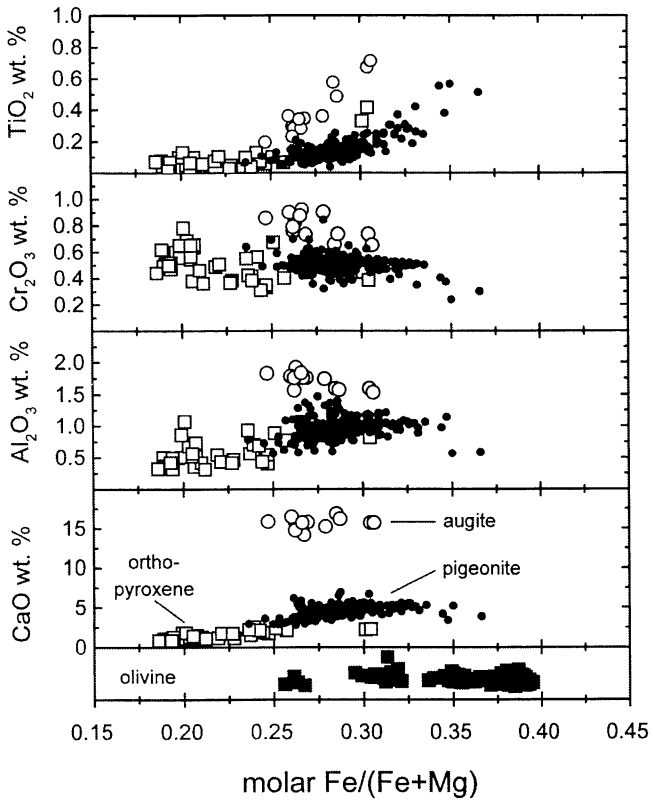

FIG. 3. Minor element variations of TiO_2, Cr_2O_3, Al_2O_3, and CaO with molar Fe/(Fe + Mg) (fe-number) in pyroxenes. Range of fe-numbers in olivine is shown for comparison. Open squares are orthopyroxene, open circles are augite, filled circles are pigeonite, and filled squares are olivine.

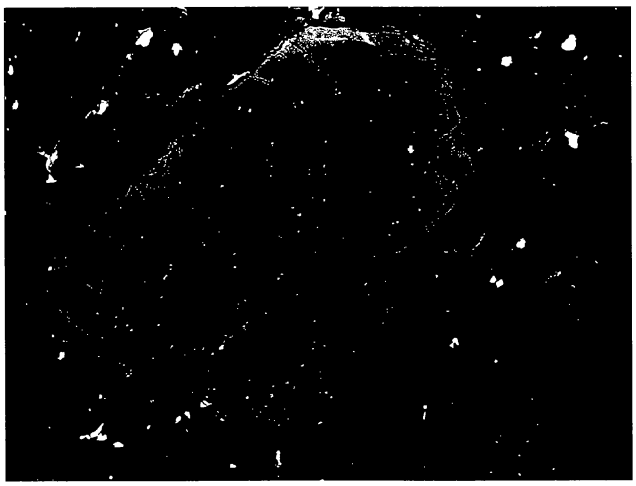

FIG. 4. Backscatter image of DaG 476 texture. Large grain in center is olivine with tiny inclusions of chromite (white). This olivine is chemically zoned from core (Fa_{26}) to rim (Fa_{38}). Cracks are filled with pigeonite and carbonate. Fine-grained groundmass consists of pyroxene (dark gray) and feldspathic glass (black) and minor FeTi-oxides and sulfide (white). Field of view is 1.6 × 1 mm.

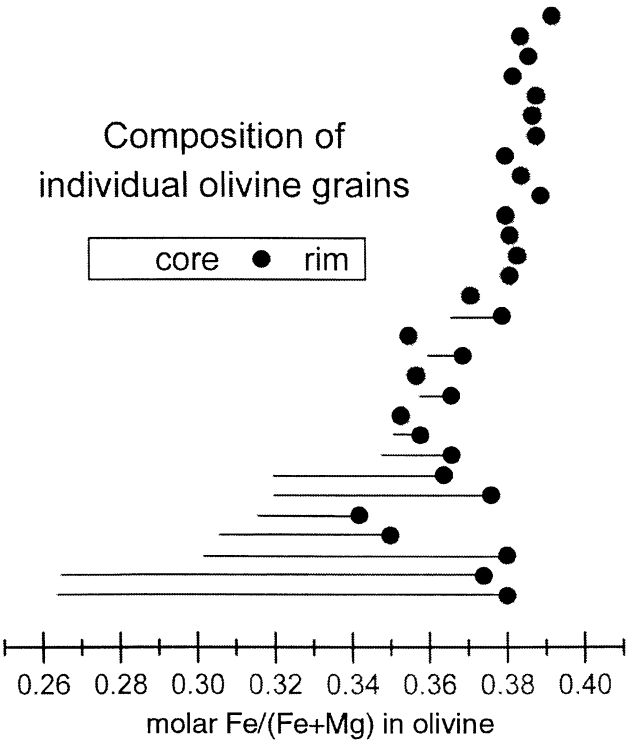

FIG. 5. Composition of core and rim pairs analyzed in individual olivine grains. Each symbol represents an average of at least two analyses. For details, see text.

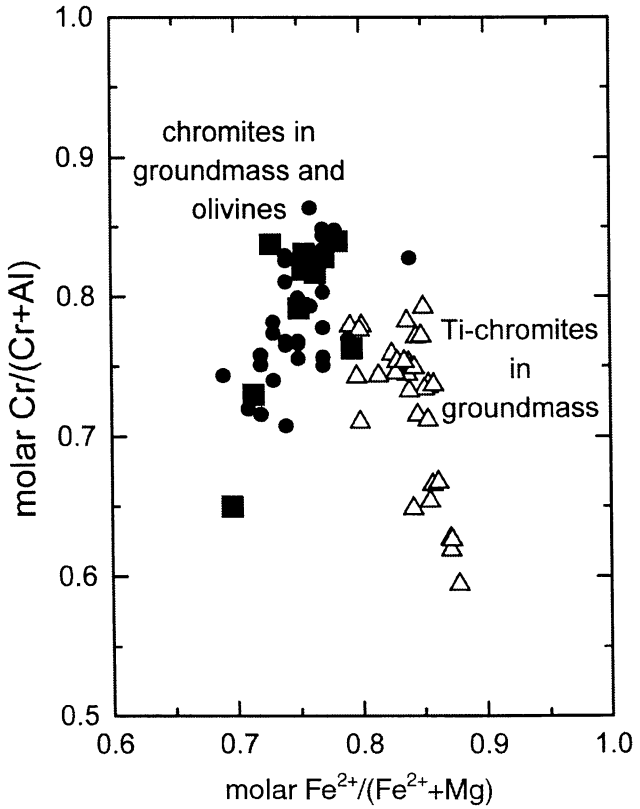

FIG. 6. Chromites have increasing Cr/(Cr + Al) ratios with increasing $Fe^{2+}/(Fe^{2+} + Mg)$. There is no compositional difference between those chromites included in olivine (black squares) and those in the groundmass (filled circles). The Ti-chromites (open triangles) are Fe-rich and have on average lower Cr/(Cr + Al) ratios.

TABLE 3. Bulk composition of DaG 476.

	Surface chip		Powder aliquots			Bulk	
	(1) INAA (66.12 mg)	s.d.%	(2) INAA (191.46 mg†)	s.d.%	(3) XRF‡ (120 + 112.5 mg)	(4) columns 2 + 3 combined	(5) $CaCO_3$ and S-free (renormalized)
wt%							
SiO_2	–	–	–	–	45.76	45.76	48.91
TiO_2*	0.38	20	0.42	12	0.39	0.39	0.42
Al_2O_3*	4.42	3	4.35	3	4.37	4.37	4.67
Cr_2O_3	0.75	3	0.78	3	0.78	0.78	0.83
FeO	16.1	3	16.1	3	16.06	16.06	17.17
MnO	0.43	3	0.42	3	0.45	0.45	0.48
MgO*	18.6	3	19.0	3	19.41	19.41	20.75
CaO*,#	8.68	5	7.25	4	7.66	5.47@	5.84
Na_2O	0.50	3	0.51	3	–	0.51	0.55
K_2O#	0.05	5	0.04	7	0.038	0.038	0.041
P_2O_5	–	–	–	–	0.32	0.32	0.34
S§,#	–	–	0.27	5	–	0.27	–
C§,#	–	–	0.47	3	–	3.92$	–
Total	–	–	–	–	95.24	97.75	100.00
ppm							
Cl	<840	–	–	–			
Sc	30.6	3	29.9	3			
V*	182	3	186	3			
Co	52.1	3	51.1	3			
Ni	220	7	300	5			
Cu	<80	–	<90	–			
Zn	51	20	66	15			
Ga	8.5	7	8.7	7			
As#	0.51	7	0.24	15			
Se	<0.9	–	0.4	30			
Br	0.72	10	1.29	7			
Rb	<4	–	<3	–			
Sb	<0.03	–	<0.03	–			
Ba#	84	15	73	10			
La	0.09	20	0.12	10			
Nd	–	–	<0.5	–			
Sm	0.31	4	0.39	7			
Eu	0.17	7	0.17	7			
Tb	0.16	15	0.20	7			
Dy	1.6	15	1.3	20			
Ho	0.2	15	0.3	15			
Yb	0.73	7	0.81	5			
Lu	0.12	5	0.13	5			
Hf	0.32	15	0.39	7			
Ta	<0.03	–	<0.02	–			
W	<0.2	–	<0.3	–			
Ir	<0.006	–	<0.0025	–			
Au	<0.001	–	0.0021	15			
Th	<0.1	–	<0.08	–			
U#	0.12	20	0.09	15			

s.d. = standard deviation in %; < upper detection limit.
*INAA data obtained by short irradiation.
†Sample weight for short irradiation 52.69 mg.
‡Unpublished data from Universität zu Köln.
§S and C analyser.
@Corrected for $CaCO_3$.
$Total C calculated as $CaCO_3$.
#Suspect to terrestrial weathering.

distinguished: $Fa_{\sim 26}$, Fa_{30} to Fa_{32}, and Fa_{34} to Fa_{36}. The absence of a smooth distribution of olivine cores compositions between Fa_{26} and Fa_{38}, which would be expected if the olivines are randomly distributed and sectioned, probably reflects the preferred alignment of olivines that is observed optically. As a result, the lowest Fa concentration of 26, analyzed in two olivine grains in one thin section only, might still not be the minimum.

Chromites, Ti-chromites, and ilmenites analyzed are characterized by high-MgO concentrations (MgO ~4.3 wt%). Composition of chromite inclusions in olivines are indistinguishable from chromites in the groundmass (Fig. 6 and Table 2). Their Cr/(Cr + Al) ratios increase with increasing $Fe^{2+}/(Fe^{2+} + Mg)$. On the other hand, Cr/(Cr + Al) ratios in Ti-chromites decrease with increasing $Fe^{2+}/(Fe^{2+} + Mg)$ ratios. Based on stochiometry, up to 13% of all Fe in chromite and Ti-chromite and up to ~5% of all Fe in ilmenite occurs as Fe^{3+}.

BULK CHEMISTRY

The results of our bulk analyses are shown in Table 3. Column 1 shows the results for a 66.1 mg chip separated from the surface of the meteorite and analyzed by INAA. Column 2 and 3 show results from INAA and XRF analyses of three splits taken from a 5 g powder aliquot. There is excellent agreement between the major elements analyzed by both methods. However, the total of 95.24 wt% for all major elements (column 3) is very low and is most likely due to the presence of weathering products. In column 4, a calculated bulk composition is shown, which combines results of XRF and INA analyses. In addition, assuming that all C is bonded in $CaCO_3$ and is a terrestrial weathering product, corrections to the bulk composition were applied. In column 4, therefore, the CaO concentration is corrected for $CaCO_3$, and all C is calculated as $CaCO_3$. This raises the total to 97.75 wt% (column 4). Other contaminants, such as sulfate (possibly gypsum and $BaSO_4$) and phyllosilicates, could account for the missing weight but their exact proportions are impossible to estimate. A sulfur and $CaCO_3$-free normalized major element composition is given in column 5 of Table 3 and listed together with other shergottites in Table 4.

Certain key element ratios are characteristic of all martian meteorites (*e.g.*, Wänke and Dreibus, 1988), reflecting geochemical similarities of these pairs of elements, and thus allow bulk planet composition estimates to be made. Among these key ratios are compatible element ratios (*e.g.*, Fe/Mn, Cr/Mg), incompatible element ratios (*e.g.*, K/La), and elements correlating with Al (*e.g.*, moderately volatile Ga and Na, and refractory Yb and Ti). The

TABLE 4. Comparison of element concentrations and ratios in shergottites.

	Basalts						Lherzolites	
	QUE 94201	EETA 79001 (B)	Shergotty	Zagami	EETA 79001 (A)	*DaG 476*	LEW 88516	ALHA 77005
References	1	2	2	2, 3	2		4	2
wt%								
MgO	6.20	7.38	9.28	11.00	16.31	20.75	25.66	27.69
Al_2O_3	12.00	9.93	7.06	5.67	5.37	4.67	2.99	2.59
CaO	11.30	10.99	10.00	10.80	7.05	5.84	4.04	3.35
TiO_2	1.80	1.12	0.87	0.77	0.64	0.42	<0.42	0.44
FeO	18.30	17.74	19.41	18.00	18.32	17.17	19.45	19.95
ppm								
S	–	1900	1330	2800*	1600	(2700)†	950	600
C	–	98	620	231*	36	(4710)†	74	82
Na	13000	12300	9570	7340	6080	4040	3640	3260
Sc	46.6	50.5	58.9	57.0	36.1	29.9	25.1	21.1
Cr	890	1250	1390	2050	4030	5700	5670	6590
Co	22.8	31.1	39.0	36.4	47.3	51.1	62.7	69.5
Ni	<20	46	83	67	158	300	250	335
Zn	130	120	83	62	81	66	70	71
Ga	27.1	24.4	14.7	14.1	12.6	8.7	8.4	7.5
Mg/(Fe + Mg) molar	0.38	0.43	0.46	0.52	0.61	0.68	0.70	0.71
Fe/Mn	41.7	39.4	37.1	36.1	39.2	35.8	41.5	43.5
K/La	1190	674	595	561	740	2810	738	700
Ga/Al	4.3	4.6	3.9	4.7	4.4	3.5	5.3	5.5
Na/Al	0.20	0.23	0.26	0.24	0.21	0.16	0.23	0.24
Na/Ti	1.20	1.83	1.84	1.59	1.59	1.62	>1.44	1.24

Dar al Gani 476 data this study, other data from (1) Dreibus *et al.* (1996), (2) Banin *et al.* (1992) and references therein, (3) Burghele *et al.* (1983), (4) Dreibus *et al.* (1992).
*Unpublished data from MPCh Mainz.
†Sulfur and C (from Table 3, column 2) are shown here only to emphasize their enrichment relative to other shergottites.

correlation of the siderophile abundances, Ni and Co, with Mg is another diagnostic feature in shergottites (Fig. 7). Based on these elemental ratios and correlations, shergottites can be distinguished from terrestrial and lunar rocks, as well as from eucrites, another group of basaltic achondrites. Dar al Gani 476 has the chemical characteristics of shergottites with respect to most of these element pairs.

Although DaG 476 is classified as a basaltic shergottite based on modal abundance of feldspathic glass, the bulk chemistry of DaG 476 indicates a strong affinity to lherzolitic shergottites (Table 4). Compared to other basaltic shergottites, it has the highest bulk mg-number (molar Mg/(Fe + Mg) = 0.68), which is only slightly lower than those of lherzolitic shergottites. The concentrations of Sc, Zn, Na, and Ga are lower, and those of Cr, Ni, and Co are higher than those of other basaltic shergottites and similar to concentrations in lherzolitic shergottites.

Ratios of Na/Al and Ga/Al in DaG 476 are lower than in other shergottites, but the Na/Ti ratio is well within their typical compositional range. Therefore, the particularly low Na/Al ratio probably reflects a slight enrichment in Al, rather than loss of the moderately volatile Na. In addition, heavy rare earth element (REE) abundances are lower than in basaltic shergottites but similar to abundances of lherzolitic shergottites. The degree of light REE fractionation is high (Sm/Nd_{CI} = >2.5, this work; Sm/Nd_{CI} = 2.56, Jagoutz *et al.*, 1999), and La abundance (La = 0.4–0.5 × CI) is very low (Fig. 8). Only QUE 94201, although it has much higher absolute REE concentrations, has a similar REE abundance pattern, indicating a relationship between these two meteorites. This is strongly supported by their Sm-Nd isotopic systematics (Jagoutz *et al.*, 1999).

The K/La ratios of the surface chip (K/La = 4610) and of the powder aliquots (K/La = 2630) are higher than typical for shergottites (K/La = 635; Wänke and Dreibus, 1988). This is due to K enrichment from terrestrial weathering, as can easily be seen in Fig. 8. Potassium concentration is a factor of 1.5 times higher in the surface sample than in the powder aliquot, which is prepared from an interior portion of the meteorite. On the other hand, CI-normalized REE abundances of both samples are identical within error, which indicates that their concentrations are not altered by terrestrial weathering. Indeed concentrations of most trace and major elements are, within error, identical in the surface and interior samples. This suggests that these elements are unaffected by weathering and also attests to the homogeneity of this meteorite.

Only concentrations of elements (*e.g.*, K, Ca, Ba, As, U), which tend to be enriched during hot desert weathering in the Dar al Gani region (Bischoff *et al.*, 1998), are higher in the surface sample (by factors of 1.2 to 2.1) than in the interior sample (Table 3, columns 1 and 2). In addition, S and particularly C concentrations are higher in DaG 476 than in other shergottites, reflecting the high degree of terrestrial alteration (Table 4). The isotopic composition of C (Wright *et al.*, 1999) supports the conclusion that it is almost entirely of terrestrial origin.

NOBLE GASES

The noble gases of DaG 476 (Table 5) are a mixture of different components. Radiogenic ^4He and ^{40}Ar are produced by the decay of U, Th, and ^{40}K, respectively. Cosmogenic nuclides are produced by the interaction of the cosmic-ray particle irradiation with meteoritic matter, and trapped gases are incorporated from the environment by several processes.

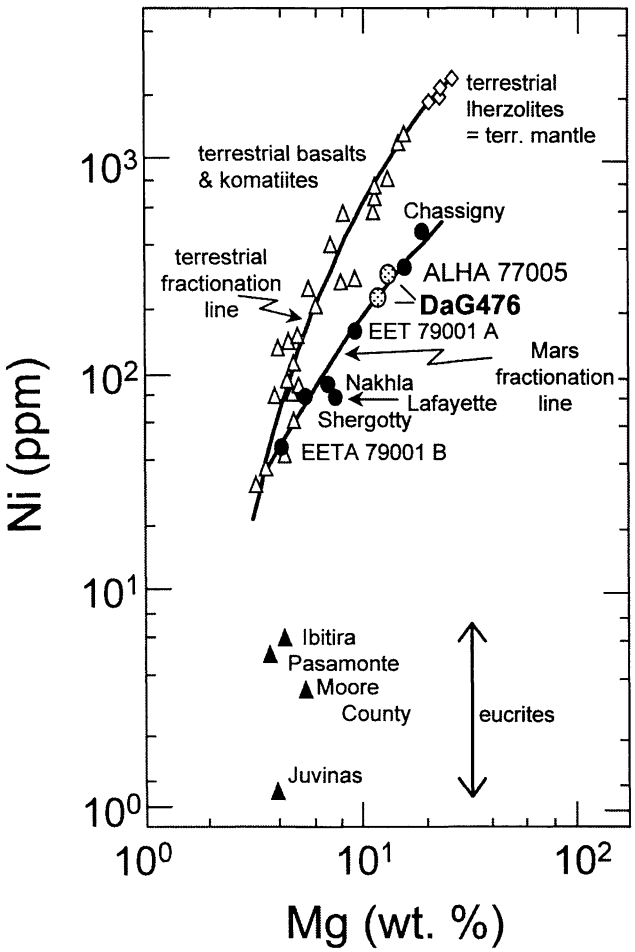

FIG. 7. Bulk rock Ni *vs.* Mg correlation of terrestrial basalts and lherzolites, martian meteorites, and eucrites. Dar al Gani 476 compositions (surface sample and powder aliquot) fall on the martian meteorite trend, intermediate between basaltic and lherzolitic shergottites. Figure modified from Wänke and Dreibus (1988).

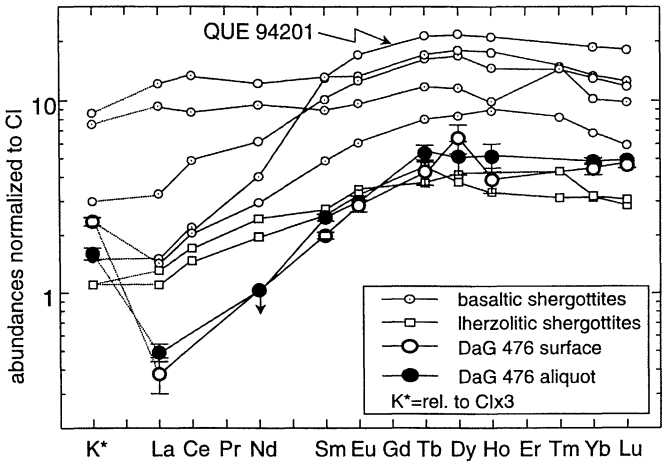

FIG. 8. The CI-normalized element abundances of K and REEs of basaltic and lherzolitic shergottites. Data sources are the same as in Table 4. Dar al Gani 476 has the lowest LREE abundances of all shergottites.

Assuming that the measured ^{40}Ar is completely of radiogenic origin and no terrestrial contamination is present, a formal K-Ar gas retention age of ~1.7 Ga is calculated using the K concentration of Table 3, column 5. This, however, is not a true "age," because martian Ar and/or terrestrial atmospheric ^{40}Ar is possibly also present in the measured samples. With the assumption that all trapped ^{36}Ar is of terrestrial contamination, the resulting K-Ar ages are 400 to 900 Ma (see Table 6). It should be noted that these numbers cannot be attributed to a special event in the history of this meteorite.

Exposure History and Ejection Age

So far five distinct ejection events have been postulated for all martian meteorites (see Eugster *et al.*, 1997). In an ongoing debate, the question arises whether just one or three impact events on Mars were responsible for delivering shergottites to Earth (Nyquist *et al.*, 1998). We have calculated the cosmic-ray exposure age of DaG 476 to contribute to this question. We assume that ^{3}He and ^{21}Ne in our measurements is completely cosmogenic. A small correction using trapped $^{20}Ne/^{22}Ne$ = 9.8 is applied to obtain the cosmogenic $^{22}Ne/^{21}Ne$ ratio that is used for the shielding correction of production rates. Cosmogenic ^{38}Ar is obtained by assuming a mixture of cosmogenic and trapped Ar with $(^{36}Ar/^{38}Ar)_c$ = 0.67 and $(^{36}Ar/^{38}Ar)_t$ = 5.00. The latter value was taken because it is between the terrestrial atmospheric value of 5.32 and a possibly lower martian ratio (see Bogard, 1997). Cosmic-ray exposure ages are calculated using production rate equations and shielding corrections given by Eugster (1988). The production rates are adjusted to the chemical composition of DaG 476 as given in Table 3. Calculated ^{3}He-, ^{21}Ne-, and ^{38}Ar-exposure ages as well as mean values are given in Table 6.

The ^{21}Ne-exposure age of DaG 476 is 1.26 ± 0.09 Ma. The ^{21}Ne-ages are generally regarded as more reliable than those calculated from ^{3}He or ^{38}Ar because the concentration of cosmogenic ^{3}He in meteorites is often lowered by diffusive loss due to solar heating in orbits with small perihelia distances; and cosmogenic ^{38}Ar, about 30 to 50% of the total ^{38}Ar in these measurements, is derived using poorly known assumptions for the isotopic abundance of the trapped component. However, the mean of all exposure ages, 1.17 ± 0.09 Ma, is within the limits of uncertainty identical to the mean ^{21}Ne-exposure age.

The relatively high $(^{22}Ne/^{21}Ne)_c$ ratio of DaG 476 is characteristic of low shielding. This is the case for small meteoroids or for meteorites with low ablation loss. In such cases, cosmogenic noble gas production rates could be influenced by solar cosmic rays.

TABLE 5. Results of the bulk measurements.*

Sample	^{3}He	^{4}He	^{20}Ne	^{21}Ne	^{22}Ne	^{36}Ar	^{38}Ar	^{40}Ar	^{84}Kr	^{132}Xe	$^{129}Xe/^{132}Xe$
DaG 476/1	1.92	15	0.38	0.26	0.31	0.53	0.17	293	0.025	0.007	1.00 ± 0.04
DaG 476/2	1.82	11	0.40	0.27	0.33	1.31	0.32	503	0.077	0.016	0.99 ± 0.06
DaG 476/3	1.61	10	0.35	0.27	0.32	1.37	0.34	450	0.075	0.014	0.99 ± 0.05
DaG 476/4	1.44	63	0.34	0.23	0.28	0.78	0.22	322	0.045	0.013	0.98 ± 0.06
DaG 476/5	2.01	11	0.36	0.29	0.34	0.75	0.22	275	0.056	0.012	0.98 ± 0.05

*Gas concentrations are given in 10^{-8} cm^3 STP/g. Uncertainties are ±5% for He, Ne, and Ar; and ±12% for Kr and Xe.

TABLE 6. Cosmogenic $(^{22}Ne/^{21}Ne)_c$ and exposure ages (in Ma) of DaG 476 as well as K-Ar ages (in Ga).*

Sample	$(^{22}Ne/^{21}Ne)_c$	T3 (Ma)	T21 (Ma)	T38 (Ma)	K-Ar (Ga)
DaG 476/1	1.201	1.2	1.21	1.1	1.4 (0.9)
DaG 476/2	1.230	1.1	1.36	1.1	2.0 (0.8)
DaG 476/3	1.200	1.0	1.24	1.1	1.9 (0.4)
DaG 476/4	1.223	0.9	1.14	1.1	1.5 (0.6)
DaG 476/5	1.204	1.2	1.35	1.3	1.4 (0.5)
Mean	1.213 ± 0.012	–	1.26 ± 0.09	–	–

*K-Ar ages are calculated assuming that all ^{40}Ar is radiogenic. Ages given in parenthesis are calculated by assuming that all ^{36}Ar is due to atmospheric contamination. Uncertainties of the calculated exposure ages are estimated to be ±20%.

However, for $(^{22}Ne/^{21}Ne)_c$ = 1.21 and a Mg/(Si + Al) ratio of 0.49, cosmogenic Ne is produced only by galactic cosmic rays according to Garrison *et al.* (1995).

The exposure age is a lower limit for the ejection age of SNC meteorites from their parent planet. Especially for Antarctic meteorites and meteorites with short exposure ages, the time spent on the Earth can be a significant component of the ejection ages. However, terrestrial ages of Saharan meteorites are generally <0.1 Ma (Wlotzka *et al.*, 1995). From the concentration of cosmogenic radionuclides, Nishiizumi *et al.* (1999) give the terrestrial age of DaG 476 to (85 ± 50) ka. Therefore, an ejection age of 1.35 ± 0.10 Ma is calculated (based on the ^{21}Ne-exposure age). This age is distinctly different from those of the two shergottite age groups that peak at ~2.8 and ~3.8 Ma (Eugster *et al.*, 1997) (Fig. 9). The ejection events of DaG 476 and EETA79001, however, are close together, and the question of a common origin as meteoroids needs further discussion.

The ejection age of EETA79001 is not well constrained. The exposure age is given as 0.65 ± 0.20 Ma (Eugster *et al.*, 1997). Terrestrial ages of this meteorite are reported as 0.012 Ma (Jull and Donahue, 1988), <0.06 Ma (Nishiizumi *et al.*, 1986), and 0.32 ± 0.17 Ma (Sarafin *et al.*, 1985). Assuming a terrestrial age of 0.32 Ma for EETA79001 yields an ejection age that is close to that of DaG 467. If one considers the short terrestrial ages only, quite different ejection ages for EETA79001 and DaG 476 are calculated. Because both meteoroids have high cosmogenic $^{22}Ne/^{21}Ne$ ratios that are indicative of small preatmospheric masses, the difference of about a factor of 2 in the concentration of cosmogenic nuclides cannot be due to shielding.

Only ~4% of the volcanic surface area of Mars appear to have the appropriate age for shergottites (Tanaka *et al.*, 1992). With a possible additional ejection event of DaG 476, the majority of meteoroid producing impacts on Mars appears to occur on a rather small fraction of its surface. This paradox remains to be explained.

Trapped Martian Gases

It has been suggested that trapped noble gases in SNC meteorites are a mixture of martian atmospheric gas and gas from the martian mantle (Ott, 1988). The mantle gas is represented by that measured in the meteorite Chassigny, whereas the martian atmospheric component is seen most prominently in glass inclusions, for example, of EETA79001 (see Garrison and Bogard, 1998).

In DaG 476, the concentrations of trapped Ne and Ar are rather low, and their isotopic composition cannot be determined from bulk measurements alone. Figure 10 shows $^{129}Xe/^{132}Xe$ *vs.* $^{84}Kr/^{132}Xe$. The position of noble gases from the Earth's atmosphere is also

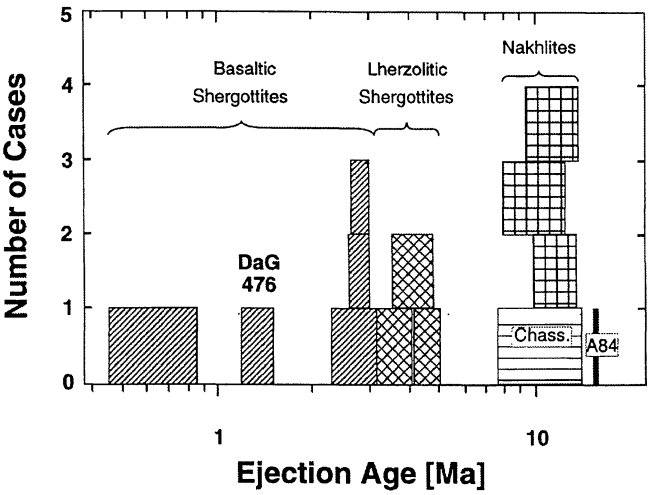

FIG. 9. Ejection ages of SNC meteorites. Basaltic shergottites, lherzolitic shergottites, nakhlites, Chassigny (Chass.), and ALH 84001 (A84) are shown with five different patterns. Boxes indicate uncertainties of ejection ages. Data from Eugster *et al.* (1997), Eugster and Polnau (1997), and Nagao *et al.* (1997).

indicated. The measurements of DaG 476 plot on a mixing line connecting Chassigny-type gas and the terrestrial atmosphere. This indicates: (1) Virtually no martian atmosphere was trapped in DaG 476 whole rock splits. (2) The low $^{129}Xe/^{132}Xe$ ratio and the $^{84}Kr/^{132}Xe$ ratios of DaG 476 are compatible with Chassigy gasses, plus a terrestrial contamination. Terrestrial contamination alone cannot explain the observed compositions, because even strongly fractionated gases in water (Scherer *et al.*, 1994) cannot account for the low Kr/Xe ratios. (3) A contribution of a terrestrial atmospheric component is commonly observed in stony meteorites from hot deserts (Scherer *et al.*, 1994) and connected to weathering products. Such products are observed as carbonate veins that follow grain boundaries and cracks.

RELATIONSHIP TO OTHER SHERGOTTITES

Shergottites comprise two rock types, basalts and lherzolites. The mineralogy of lherzolitic shergottites is dominated by olivine.

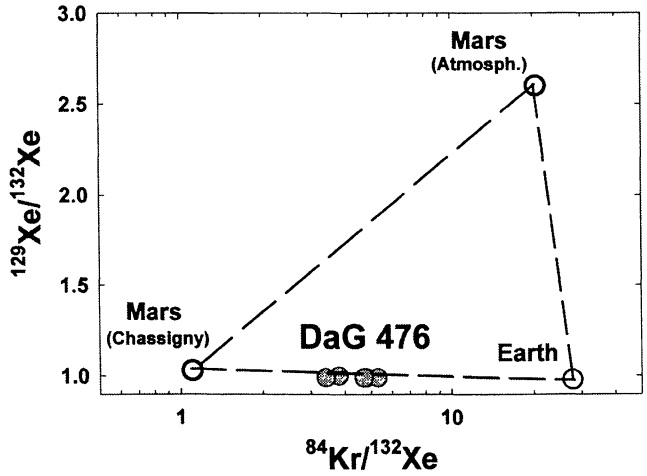

FIG. 10. Three-isotope plot of $^{129}Xe/^{132}Xe$ *vs.* $^{84}Kr/^{132}Xe$ for SNC meteorites. The DaG 476 measurements lie on the mixing line between martian mantle gas (Chassigny) and the terrestrial atmosphere indicating atmospheric contamination.

These rocks have a cumulate texture and probably formed in a closed system (magma chamber) in a plutonic environment (Harvey *et al.*, 1993). Basaltic shergottites are relatively fine-grained and consist predominantly of clinopyroxene and feldspathic glass. Their mineral chemistry indicates that most of them do not represent pure liquid compositions but rather are liquids contaminated to various degrees with cumulus pyroxene (Stolper and McSween, 1979). Only basaltic shergottite QUE 94201 is believed to represent a melt composition (McSween *et al.*, 1996).

Texture and grain size, as well as mineralogy (with the exception of excess olivine, orthopyroxene, and chromite) of DaG 476 are similar to those of basaltic shergottites. Among the known basaltic shergottites, DaG 476 is the most magnesian member. Its mineral compositions and bulk chemistry are, to a first approximation, intermediate between those of lherzolitic and basaltic shergottites.

With respect to the phases present, the closest analogue among basaltic shergottites is lithology A of EETA79001 (EETA79001(A)). Lithology A is unusual among basaltic shergottites in that it contains olivine, orthopyroxene, and chromite. In EETA79001(A), these minerals form clusters, which are interpreted as xenoliths. The observation that they do not form clusters in DaG 476 suggests that they may be phenocrysts. In addition, bulk chemistry and mineralogy of EETA79001(A) and DaG 476 are distinct in that the latter is more magnesian. This is reflected in its low bulk Fe concentration and the Mg-rich compositions of oxides, pigeonites, and augites, which do not extend to fe-numbers as high as those in EETA79001(A) pyroxenes. Also, the lower REE abundances and a strong depletion in LREEs imply that DaG 476 is derived from a source different in composition to EETA79001(A).

FORMATION OF DAR AL GANI 476

The origin of olivine, orthopyroxene, and chromite is crucial to understanding the formation of DaG 476. Four possibilities for their origin are considered: (1) formation as early phenocrysts in a closed system either from a parent magma or from an impact melt, (2) formation as cumulates from model shergottite parent magma compositions, (3) incorporation as xenoliths that were subsequently disaggregated, or (4) formation as phenocrysts in a lherzolitic melt that then mixes with a basaltic melt.

The textures of these phases indicate that they could be early phenocrysts crystallizing in a closed system from a melt of a DaG 476 bulk-like composition. Such a magma composition is more magnesian than those of other shergottite parent magmas, as derived by several models (*e.g.*, Longhi and Pan, 1989). Therefore, either the parent magma composition of DaG 476 is very unusual, or alternatively, the melt formed by impact melting.

The bulk composition of DaG 476 is only consistent with previous models for shergottite parent magma compositions if magnesian phases in DaG 476 are cumulus. However, compositions of even the most ferroan augites and pigeonites in DaG 476 barely overlap with compositions of their least ferroan counterparts in other basaltic shergottites. Therefore, the melt from which DaG 476 augite and pigeonite crystallized must have been more magnesian than the melt which produced the most magnesian cores of these phases in Shergotty, Zagami, and lithology B of EETA79001. This observation argues against a model where DaG 476 crystallized from a typical parent magma composition as a cumulate.

Another possibility is that these phases represent relics of disaggregated xenoliths, as in EETA79001(A) (McSween and Jarosewich, 1983), which were incorporated and partially assimilated by a basaltic melt. In this scenario, melting of olivine and chromite would have been minor, and both phases would have been evenly dispersed in the groundmass. Orthopyroxene grains, which are restricted to pyroxene cores and are mantled by pigeonite, would be relics of grains mostly assimilated by the melt. Faster diffusion of Mg and Fe in olivine and chromite could explain why they are more in equilibrium with groundmass pigeonite and augite compositions than with Mg-rich orthopyroxenes. This model seems unlikely, because there is no textural evidence for a xenolithic origin of these phases in DaG 476. In addition, mixing calculations show that a calculated groundmass composition of DaG 476 (*i.e.*, bulk composition minus the weight proportions of olivine, orthopyroxene, and chromite) has the same mg-number as the bulk (Table 7). Calculated proportions of mafic minerals assimilated by such a groundmass are about 43–48 wt% orthopyroxene, about 2–3 wt% olivine, and ~1 wt% chromite. Although this is in agreement with the petrographic observation that olivine–orthopyroxene–chromite clusters are absent in DaG 476, it seems unlikely that only orthopyroxene is assimilated by the melt.

The fourth possibility is analogous to a model suggested for formation of EETA79001(A) by Wadhwa *et al.* (1994). However, DaG 476 cannot have formed by a simple mixing process of lherzolitic melt with a basaltic melt, because concentrations of major elements (Fe and Ti) as well as concentrations of LREEs in DaG 476 are significantly lower than in known shergottites (Fig. 8 and Table 4).

As discussed above, possibilities (2) and (4) can be ruled out for the origin of DaG 476. Possibility (3) is still an option, although the physical problem—already pointed out for EETA79001(A)—that a fractionated melt has to assimilate ultramafic material persists, unless the melt is superheated by a few hundred degrees (McSween and Jarosewich, 1983; Wadhwa *et al.*, 1994; Mittlefehldt *et al.*, 1999). Detailed thermodynamic calculations are required to solve this question.

TABLE 7. Calculated groundmass composition and mixing calculations results.

	DaG 476 bulk†	DaG 476 groundmass‡	Residuals* groundmass *a*	Residuals* groundmass *b*
SiO_2	48.91	50.95	0.11	0.19
MgO	20.75	18.32	–0.24	–0.45
FeO	17.17	15.46	0.14	0.28
Al_2O_3	4.67	5.66	0.43	–0.20
MnO	0.48	0.47	–0.02	0
Cr_2O_3	0.83	0.92	–0.13	–0.08
Na_2O	0.55	0.67	0.20	0.23
TiO_2	0.42	0.51	0.41	0.18
CaO	5.84	7.04	–1.12	–0.88
molar Mg/(Mg + Fe)	0.68	0.68	–	–

DaG 476 groundmass	wt%		wt%
QUE 94201	49	EETA79001(B)	53
olivine	2	olivine	3
opx	48	opx	43
chromite	0.9	chromite	1

†Bulk composition from Table 3, column 5.
‡Groundmass is calculated by subtracting 15 wt% olivine (Fa_{32}), 3 wt% orthopyroxene ($Fs_{18}Wo_{1.6}$), and 1 wt% chromite (mg-number = 0.22).
*Residuals indicate the match between the mixing calculation composition and DaG 476 groundmass composition, depending on whether the basaltic melt composition was assumed to be *a* = QUE 94201 (Dreibus *et al.*, 1996) or *b* = EETA79001(B) (McSween and Jarosewich, 1983).

Alternatively, it has been suggested that melting triggered by a large impact might provide the needed heat (Mittlefehldt *et al.*, 1999). In order to explain the magnesian phases in DaG 476 as xenocrysts, however, the impact is required to produce a magma body large enough that convection is possible, so that unresorbed grains of olivine and chromites could have been thoroughly mixed with the melt at least on a centimeter-scale. This is required from the relatively homogeneous bulk composition of DaG 476.

This leaves open possibility (1) that these phases indeed are phenocrysts from a melt of DaG 476 bulk-like composition. This melt could have had an impact origin which, in contrast to the model above, led to complete melting and upon cooling to crystallization of olivine, orthopyroxene, and chromites as phenocrysts. However, this melt could also represent a shergottite parent magma, albeit of unusual composition, because chemically it is related to compositions of known shergottites.

SUMMARY

Dar al Gani 476 is classified as a basaltic shergottite based on its mineralogy. It has a fine-grained groundmass consisting of clinopyroxene, pigeonite and augite, feldspathic glass and chromite, Ti-chromite, ilmenite, sulfides, and whitlockite. Isolated olivine and single chromite grains occur in the groundmass. Orthopyroxene forms cores of some pigeonite grains. Shock-features, such as shock-twinning, mosaicism, cracks, and impact-melt pockets, are abundant. Severe weathering in the Sahara led to significant formation of carbonate veins crosscutting the entire meteorite.

Dar al Gani 476 is distinct from other known shergottites. Chemically, it is the most magnesian member among known basaltic shergottites and intermediate in composition for most trace and major elements between lherzolitic and basaltic shergottites. Unique are the very low bulk REE element abundances. The CI-normalized abundances of LREEs are even lower than those of lherzolitic shergottites. The overall abundance pattern, however, is similar to that of QUE 94201.

Textural evidence indicates that orthopyroxene, as well as olivine and chromite, crystallized as phenocrysts from a magma similar in composition to that of bulk DaG 476. Whether such a magma composition can be a shergottite parent melt or was formed by impact melting needs to be explored further. At this time, it cannot entirely be ruled out that these phases represent relics of disaggregated xenoliths that were incorporated and partially assimilated by a basaltic melt, although the texture does not support this possibility.

Trapped noble gas concentrations are low and dominated by a Chassigny-like mantle component. Virtually no martian atmosphere was trapped in DaG 476 whole-rock splits. The exposure age of 1.26 ± 0.09 Ma is younger than that of most shergottites and closer to that of EETA79001. The ejection age of 1.35 ± 0.1 Ma could mark another distinct impact event.

Acknowledgements–The authors are greatly indebted to H. Palme and D. Wolf, Institut für Mineralogie und Geochemie, Universität zu Köln, for providing their unpublished XRF data. They also thank R. Haubold for analyzing S and C. The authors thank for help and assistance with the electron microprobe, K. Kadisch, E. Macsenaere, and B. Schulz-Dobrick (Johannes-Gutenberg-Universität Mainz, Mineralogie), and A. Greshake (Humboldt-Universität, Berlin). One of the authors, J. Zipfel, especially wants to thank C. A. Goodrich and E. Jagoutz for their stimulating thoughts and discussion about SNC meteorites. We thank M. Ebihara, R. P. Harvey, D. W. Mittlefehldt, and T. D. Swindle for thoughtful reviews. Comments of the reviewers and of C. A. Goodrich had a major impact on the grammar and style of this paper.

Editorial handling: D. W. Mittlefehldt

REFERENCES

BANIN A., CLARK B. C. AND WÄNKE H. (1992) Surface chemistry and Mineralogy. In *Mars* (eds. H. H. Kiefer, B. M. Jakosky, C. W. Snyder and M. S. Matthews), pp. 594–625. Univ. Arizona Press, Tucson, Arizona, USA.

BISCHOFF ET AL. (1998) Petrology, chemistry, and isotopic composition of the lunar highland regolith breccias Dar al Gani 262. *Meteorit. Planet. Sci.* **33,** 1243–1257.

BOGARD D. D. (1997) A reappraisal of the Martian $^{36}Ar/^{38}Ar$ ratio. *J. Geophys. Res.* **102,** 1653–1661.

BOGARD D. D. AND JOHNSON P. (1983) Martian gases in an Antarctic meteorite. *Science* **221,** 651–654.

BURGHELE A., DREIBUS G., PALME H., RAMMENSEE W., SPETTEL B., WECKWERTH G. AND WÄNKE H. (1983) Chemistry of shergottites and the shergotty parent body (SPB): Further evidence for the two component model of planet formation (abstract). *Lunar Planet. Sci.* **14,** 80–81.

DREIBUS G., JOCHUM K. H., PALME H., SPETTEL B., WLOTZKA F. AND WÄNKE H. (1992) LEW88516: A meteorite compositionally close to the "Martian mantle" (abstract). *Meteoritics* **27,** 216–217.

DREIBUS G., PALME H., SPETTEL B., ZIPFEL J. AND WÄNKE H. (1995) Sulfur and selenium in chondritic meteorites. *Meteoritics* **30,** 439–445.

DREIBUS G., SPETTEL B., WLOTZKA F., SCHULTZ L., WEBER H. W., JOCHUM K. P. AND WÄNKE H. (1996) QUE 94201: An unusual Martian basalt (abstract). *Meteorit. Planet. Sci.* **31 (Suppl.),** A39–A40.

EUGSTER O. (1988) Cosmic-ray production rates for ^{3}He, ^{21}Ne, ^{38}Ar, ^{83}Kr, and ^{126}Xe in chondrites based on ^{81}Kr-Kr exposure ages. *Geochim. Cosmochim. Acta* **52,** 1649–1659.

EUGSTER O. AND POLNAU E. (1997) Mars–Earth transfer time of lherzolithe Yamato 793605. *Antarc. Meteorite Res.* **10,** 143–149.

EUGSTER O., WEIGEL A. AND POLNAU E. (1997) Ejection times of Martian meteorites. *Geochim. Cosmochim. Acta* **61,** 2749–2757.

FOLCO L., FRANCHI I. A., SCHERER P., SCHULTZ L. AND PILLINGER C. T. (1999) Dar al Gani 489 basaltic shergottite: A new find from the Sahara likely paired with Dar al Gani 476 (abstract). *Meteorit. Planet. Sci.* **34 (Suppl.),** A36–A37.

GARRISON D. H. AND BOGARD D. D. (1998) Isotopic composition of trapped and cosmogenic noble gases in several Martian meteorites. *Meteorit. Planet. Sci.* **33,** 721–736.

GARRISON D. H., RAO M. N. AND BOGARD D. D. (1995) Solar-proton produced neon in shergottite meteorites and implications for their origin. *Meteoritics* **30,** 738–747.

HARVEY R. P., WADHWA M., MCSWEEN H. Y., JR. AND G. CROZAZ (1993) Petrography, mineral chemistry, and petrogenesis of Antarctic Shergottite LEW88516. *Geochim. Cosmochim. Acta* **57,** 4769–4783.

JAGOUTZ E., BOGDANOVSKI O., KRESTINA N. AND JOTTER R. (1999) DaG: A new age in the SNC family, or the first gathering of relatives (abstract). *Lunar Planet. Sci.* **30,** #1808, Lunar Planetary Institute, Houston, Texas, USA (CD-ROM).

JULL A. J. T. AND DONAHUE D. J. (1988) Terrestrial ^{14}C age of the Antarctic shergotite EETA79001. *Geochim. Cosmochim. Acta* **52,** 1309–1311.

LINDSLEY D. (1983) Pyroxene thermometry. *Am. Mineral.* **68,** 477–493.

LOEKEN T., SCHERER P., WEBER H. W. AND SCHULTZ L. (1992) Noble gases in eighteen stone meteorites. *Chem. Erde* **52,** 249–259.

LONGHI J. AND PAN V. (1989) The parent magmas of the SNC meteorites. *Proc. Lunar Planet. Sci. Conf.* **19th,** 451–464.

LUNDBERG L. L., CROZAZ G. AND MCSWEEN H. Y., JR. (1990) Rare earth elements in minerals of the ALHA77005 shergottite and implications for its parent magma and crystallization history. *Geochim. Cosmochim. Acta* **54,** 2535–2547.

MCCOY T. J., WADHWA M. AND KEIL K. (1999) New lithologies in the Zagami meteorite: Evidence for fractional crystallization of a single magma unit on Mars. *Geochim. Cosmochim. Acta* **63,** 1249–1262.

MCKAY D. S., GIBSON E. K., JR., THOMAS-KEPRTA K. L., VALI H., ROMANEK C. S., CLEMETT S. J., CHILLIER X. D. F., MAECHLING C. R. AND ZARE R. N. (1996) Search for life on Mars: Possible relic biogenic activity in Martian meteorite ALH84001. *Science* **273,** 924–930.

MCKAY D. S., WENTWORTH S. W., THOMAS-KEPRTA K., WESTALL F. AND GIBSON E. K., JR. (1999) Possible Bacteria in Nakhla (abstract). *Lunar Planet. Sci.* **30,** #1816, Lunar Planetary Institute, Houston, Texas, USA (CD-ROM).

MCSWEEN H. Y., JR. (1994) What we have learned about Mars from SNC meteorites. *Meteoritics* **29,** 757–779.

MCSWEEN H. Y., JR. AND JAROSEWICH E. (1983) Petrogenesis of the Elephant Moraine A79001 meteorite: Multiple magma pulses on the shergottite parent body. *Geochim. Cosmochim. Acta* **47,** 1501–1513.

MCSWEEN H. Y., JR., STOLPER E. M., TAYLOR L. A., MUNTEAN R. A.,

O'KELLEY G. D., ELDRIDGE J. S., BISWAS S., NGO H. T. AND LIPSCHUTZ M. E. (1979) Petrogenetic relationship between Allan Hills 77005 and other achondrites. *Earth Planet. Sci. Lett.* **45,** 275–284.

MCSWEEN H. Y., JR., EISENHOUR D. D., TAYLOR L. A., WADHWA M. AND CROZAZ, G. (1996) QUE 94201 shergottite: Crystallization of a Martian basaltic magma. *Geochim. Cosmochim. Acta* **60,** 4563–4569.

MIKOUCHI T. (1999) Preliminary examination of Dar al Gani 476: A new basaltic martian meteorite similar to lithology A of EETA79001 (abstract). *Lunar Planet. Sci.* **30,** #1557, Lunar Planetary Institute, Houston, Texas, USA (CD-ROM).

MITTLEFEHLDT D. W., LINDSTROM D. J., LINDSTROM M. M. AND MARTINEZ R. R. (1999) An impact-melt origin for lithology A of martian meteorite Elephant Moraine A79001. *Meteorit. Planet. Sci.* **34,** 357–367.

NAGAO K., NAKAMURA T., MIURA Y. N. AND TAKAOKA N. (1997) Noble gases and mineralogy of primary igneous materials of the Yamato 793605 shergottite. *Antarc. Meteorite Res.* **10,** 125–142.

NISHIIZUMI K., KLEIN J., MIDDLETON R., ELMORE D., KUBIK P. W. AND ARNOLD J. R. (1986) Exposure history of shergottites. *Geochim. Cosmochim. Acta* **50,** 1017–1021.

NISHIIZUMI K., MASARIK J., WELTEN K. C., CAFFEE M. W., JULL A. J. T. AND KLANDERUD S. E. (1999) Exposure history of new Martian meteorite Dar al Gani 476 (abstract). *Lunar Planet. Sci.* **30,** #1966, Lunar Planetary Institute, Houston, Texas, USA (CD-ROM).

NYQUIST L. E., BORG L. E. AND SHIH C. K. (1998) The shergotty age paradox and the relative probabilities for Martian meteorites of differing ages. *J. Geophys. Res.* **103,** 31 445–31 455.

OTT U. (1988) Noble gases in SNC meteorites: Shergotty, Nakhla, Chassigny. *Geochim. Cosmochim. Acta* **52,** 1937–1948.

SARAFIN ET AL. (1985) ^{10}Be, ^{26}Al, ^{53}Mn and light noble gass in the Antarctic shergottite EETA79001(A). *Earth Planet. Sci. Lett.* **75,** 72–76.

SCHERER P., SCHULTZ L. AND LOEKEN T. (1994) Weathering and atmospheric noble gases in chondrites. In *Noble Gas Geochemistry and Cosmochemistry* (ed. J. Matsuda), pp. 43–53. Terra Sci. Publ. Comp., Tokyo, Japan.

STEELE I. M. AND SMITH J. V. (1982) Petrography and mineralogy of two basalts and olivine–pyroxene–spinel fragments in achondrite EETA 79001. *Proc. Lunar Planet. Sci. Conf.* **13th,** *J. Geophys. Res.* **87,** A375–A384.

STOLPER E. AND MCSWEEN H. Y., JR. (1979) Petrology and origin of the shergottite meteorites. *Geochim. Cosmochim. Acta* **43,** 1475–1498.

TANAKA K. L., SCOTT D. H. AND GREELEY R. (1992) 11. Global stratigraphy. In *Mars* (eds. H. H. Kiefer, B. M. Jakosky, C. W. Snyder and M. S. Matthews), pp. 345–382. Univ. Arizona Press, Tucson, Arizona, USA.

TREIMAN A. H., MCKAY G. A., BOGARD D. D., MITTLEFEHLDT D. W., WANG M-S., KELLER L., LIPSCHUTZ M. E., LINDSTROM M. M. AND GARRISON D. (1994) Comparison of the LEW88516 and ALHA77005 martian meteorites: Similar but distinct. *Meteoritics* **29,** 581–592.

WADHWA M., MCSWEEN H. Y., JR. AND CROZAZ G. (1994) Petrogenesis of shergottite meteorites inferred from minor and trace element microdistributions. *Geochim. Cosmochim. Acta* **58,** 4213–4229.

WÄNKE H. AND DREIBUS G. (1988) Chemical composition and accretion history of terrestrial planets. *Phil. Trans. Royal Soc. London* **A 325,** 545–557.

WIENS R. C., BECKER R. H. AND PEPIN R. O. (1986) The case for a martian origin of the shergottites. II. Trapped and indigenous gas components in EETA 79001 glass. *Earth Planet. Sci. Lett.* **77,** 149–158.

WLOTZKA F., JULL A. J. T. AND DONAHUE D. J. (1995) Carbon-14 terrestrial ages of meteorites from Acfer, Algeria. In *Workshop on Meteorites from Cold and Hot Deserts* (eds. L. Schultz, J. O. Annexstad and M. E. Zolensky), pp. 72–73. LPI Techn. Rep. 95-02, Houston, Texas, USA.

WRIGHT I. P., FRANCHI I. A., GRADY M. M. AND PILLINGER C. T. (1999) Dar al Gani 476—Lucky for some, unlucky for others (abstract). *Lunar Planet. Sci.* **30,** #1594, Lunar Planetary Institute, Houston, Texas, USA (CD-ROM).

ZIPFEL J., SPETTEL B., PALME H. AND DREIBUS G. (1999) Petrology and chemistry of Dar al Gani 476, a new basaltic shergottite (abstract). *Lunar Planet. Sci.* **30,** #1206, Lunar Planetary Institute, Houston, Texas, USA (CD-ROM).